9-27-77
27
25 to NTIS

UCID- 17582

Lawrence Livermore Laboratory

EFFECTS OF BEAT-WAVE ELECTRON TRAPPING ON STIMULATED RAMAN AND THOMSON SCATTERING

Bruce I. Cohen and Allan N. Kaufman

September 13, 1977

MASTER

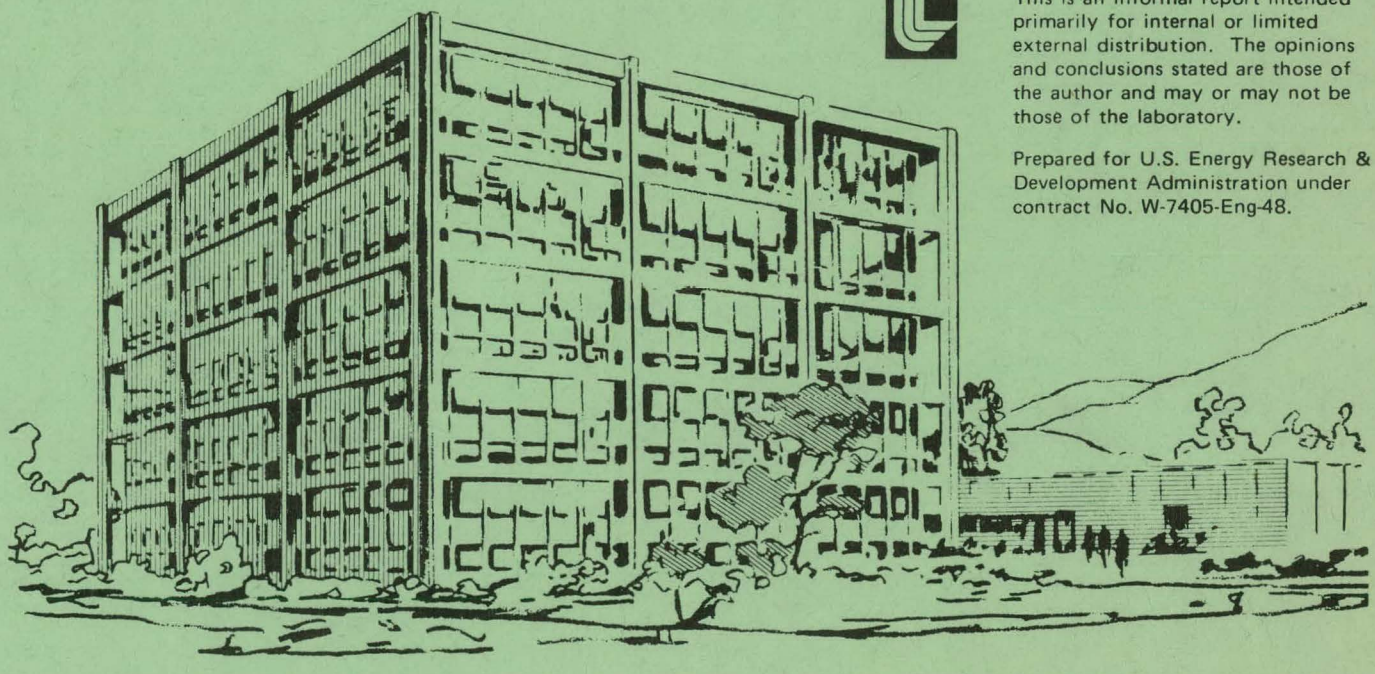

Prepared for U.S. Energy Research & Development Administration under contract No. W-7405-Eng-48.

DISCLAIMER

EFFECTS OF BEAT-WAVE ELECTRON TRAPPING ON STIMULATED RAMAN AND THOMSON SCATTERING

Bruce I. Cohen

Lawrence Livermore Laboratory, University of California
Livermore, California 94550

and

Physics Department and Lawrence Berkeley Laboratory
University of California, Berkeley, California 94720

and

Allan N. Kaufman

Physics Department and Lawrence Berkeley Laboratory
University of California, Berkeley, California 94720

ABSTRACT

The influence of electron trapping on a large amplitude plasma oscillation driven by the nonlinear interaction of two electromagnetic waves (stimulated Raman scattering) is studied analytically and by means of numerical simulation. When the plasma oscillation is resonantly excited to sufficiently large amplitude and electron trapping occurs, there ensues considerable modification of the electron velocity distribution function. The stimulated scattering ceases to be a resonant three-wave process but continues as induced scattering by resonant electrons (stimulated Thomson scattering).

I. Introduction

The nonlinear processes known as three-wave decay and induced scattering are closely related. The present study shows how particle trapping can cause the former process to evolve into the latter.

To be specific, we consider two electromagnetic plasma waves (ω_1, ω_2) subject to the decay process, whereby the ponderomotive potential at the beat frequency ($\omega_1 - \omega_2 \equiv \omega_0$) drives a Langmuir wave ($\omega_0 \approx \omega_p$), thereby inducing Raman decay. This process has been extensively studied in many contexts,[1-14] but the waves have usually been treated as being of small amplitude. When one of the waves (the Langmuir wave) is of sufficiently large amplitude so as to trap electrons, the process is greatly modified. In a previous paper,[15] we developed analytical tools for interpreting computer-simulation results of the process, by considering the more tractable model where the electromagnetic-wave amplitudes were held fixed. Our conclusions from that study will be discussed in the following section, as an introduction to the present study in which those amplitudes evolve appropriately from the nonlinear wave coupling.

In the course of the three-wave decay, energy is deposited irreversibly into the plasma electrons by trapping. The consequent increase in electron kinetic energy and momentum changes the plasma response, at the beat frequency, from being a nearly resonant collective wave (resonance meaning $\omega_1 - \omega_2 \approx \omega_p$) to being a non-collective particle resonance [$\omega_1 - \omega_2 \approx (\vec{k}_1 - \vec{k}_2) \cdot \vec{v}$]. Such a response is sometimes described as a "quasi-mode," and the associated electromagnetic-wave evolution is called induced scattering.[5,16-19]

In Section II, we shall review prior studies of three-wave decay, as they relate to the present work, and shall discuss our conclusions from our previous paper.[15] In Section III, we present the analytical theory associated with the nonlinear process under investigation. The electromagnetic waves and their coupling are adequately treated by a cold-fluid model, but the beat-wave response demands a fully kinetic treatment. Since the latter is not yet amenable to analytic solution, computer simulation is used to study the process. Section IV is devoted to a presentation of simulation results and to their detailed interpretation. The final section summarizes our conclusions and discusses practical implications.

II. Literature Survey

Three-wave interactions are encountered in many branches of physics. Consequently, there is a large literature associated with the study of these processes. We shall draw attention to a number of papers[1-38] which are relevant to the present discussion, but shall review Reference 15 in some detail because of its specific interest to this study.

Much of the early work on stimulated scattering of electromagnetic waves has come from researchers in solid-state physics and nonlinear optics.[1-4,20,22] Many classic papers on three-wave interactions have been written by workers in those fields. An apparently universal feature of these processes is the emergence of a Manley-Rowe condition.[22-26] Generally speaking, the Manley-Rowe condition can be formulated as a conservation law for wave action or quanta. Our present study illustrates

how the wave action of two of the waves participating in a three-wave decay or induced scattering is conserved independent of the details of the dynamics of the third wave (Langmuir wave) or quasi-mode involved. The Manley-Rowe condition dictates important constraints on the energy and momentum transferred in these processes.

The linear aspects of three-wave interactions and induced scattering, so-called parametric instabilities, have been recently reviewed in Reference 21. A particularly comprehensive study of the parametric instabilities associated with the stimulated scattering of electromagnetic waves in a homogeneous, unmagnetized plasma appears in Reference 5. The calculation of the nonlinear aspects of three-waves interactions have evolved from the early considerations of Sagdeev and Galeev,[27] describing the cyclic behavior of three coupled modes in the absence of dissipation, to the use of the sophisticated inverse scattering method,[28] which has allowed the space-time description of coupled, convecting pulses. Recently, Reiman, Bers, and Kaup have extended the application of the latter method to the solution of coupled modes with no linear dissipation in an inhomogeneous medium.[29]

The three-wave decay ceases to be reversible when the waves are subject to dissipation (or instability). There have been many interesting studies of the influence of linear dissipation on three-wave interactions in both homogeneous and inhomogeneous media.[9-12,30,31] The present work deals with a specific example of irreversible three-wave decay in which there is (nonlinear) dissipation owing to a wave-particle resonance and trapping. When the damping is severe the three-way interaction is described as

nonlinear Landau damping or induced scattering.[5,16-19] Litvak and Trakhtengerts,[16] Johnston,[18] and Johnston and Kulsrud[19] have contributed important papers on induced scattering. The further decay of a decay-product wave can also provide the initial decay process a source of dissipation. This is called multiple scattering[32] or cascading.[7]

Our own work[7,9,11,12,15,38] in this area has been partially motivated by the possibility of using stimulated scattering as a means of heating a plasma with lasers. Beat heating and optical mixing have been areas of active research for some time.[6-12,33-38] Reference 38 contains a review of research on various aspects of beat heating in homogeneous or inhomogeneous plasmas, and for linear and nonlinear beat-wave. The present study and Reference 15 are outgrowths of Reference 38, and address themselves to the effects of trapped particles on beat heating. In Reference 38 are presented quantitative arguments supporting the possibility of electron trapping in plasma waves resonantly excited by the beating of CO_2 lasers in a θ-pinch plasma. The present study and that of Reference 15 also analyze the more fundamental problem of driven nonlinear plasma waves. While there has been considerable study of nonlinear, freely propagating plasma waves,[39-41] much less attention has been given to the driven case.[15,42,43]

In order to follow the nonlinear orbit modifications of the electrons in their own self-consistent longitudinal fields, we have performed computer simulations describing the evolution of the scattering. The authors of References 13,14, and 17 have also numerically simulated the effects of trapping on induced scattering and Raman scattering. Litvak

Petrukhina, and Trakhtengerts studied the induced scattering of two transverse waves by resonant particles.[17] Their numerical calculations exclude plasma collective effects, i.e., the self-consistent Coulomb potential is ignored. We include collective effects in our simulations by solving Poisson's equation in order to examine Raman and induced scattering together.

We also extend the work of Forslund, Kindel, and Lindman[13] and of Klein, Ott, and Manheimer,[14] who considered the nonlinear saturation of stimulated Raman scattering due to electron trapping. Out study differs in various respects. We have chosen the initial amplitudes of the electromagnetic waves to be comparable. This serves to immediately excite a large amplitude plasma wave which rapidly traps electrons. We can therefore ignore ion effects which presumably occur on a much longer time scale.[38] We then follow the scattering over many bounce periods of the trapped electrons in order to examine the long-term evolution of the scattering process and the substantial modification of the electron velocity distribution function which occurs.

This paper is the logical conclusion of our earlier study described in Reference 15. This earlier work focused on the nonlinear plasma response to resonant excitation near the electron plasma frequency by a constant amplitude, finite-wavelength, external force. The exciting field represented a ponderomotive force, and the principal nonlinear feature of the plasma response was particle trapping. The nonlinear dielectric response of the plasma was described in terms of a nonlinear frequency shift and a dissipation rate. The effects of trapped particles were analyzed in detail.

In our simulations, large negative frequency shifts, due to extensive trapping, were observed, with a time-dependent damping rate initially in excess of that predicted by linear theory (Figures 2 and 4 of Refernce 15). The frequency mismatch between the ponderomotive driving frequency and the nonlinear normal mode frequency gave rise to a modulation of the amplitude and phase of the plasma response. Particle trapping produced further modulation at a higher frequency, the trapped-particle bounce frequency. Energy and momentum conservation laws were presented which illustrated the relationships of the nonlinear phenomena.

The present study extends the calculation of Reference 15 by including the self-consistent determination of the ponderomotive force for stimulated Raman and Thomson scattering. We shall analyze the evolution of the electromagnetic-wave amplitudes and the plasma modification by again utilizing the concept of a nonlinear dielectric function. We also introduce the hybrid simulation of the scattering, wherein coupled-mode equations describing the electromagnetic waves are combined with a one-dimensional electrostatic particle code.[44]

Many of the features observed in the simulations in Reference 15 are also found here. However, because the ponderomotive force is now calculated self-consistently and not held constant, there is a finite amount of energy available to the electromagnetic waves and the plasma. We observe appreciable depletion of the higher frequency transverse wave and consequent plasma heating. Because of nonlinear effects, the excited electron plasma wave becomes heavily damped; and induced scattering supercedes Raman decay. Our results are thus particularly relevant to the understanding of trapping effects on beat heating[7-12] and on optical mixing for use as a plasma-laser

amplifier.[45] Similar nonlinear effects should be important in schemes proposed for the generation of microwaves by relativistic electron beams[46,47] and for the free-electron laser,[48] which also employ stimulated scattering processes.

III. Theoretical Formulation

For the sake of simplicity we consider an unmagnetized, uniform electron plasma of warm, mobile electrons with a fixed, neutralizing ion background. Furthermore, we treat the transverse wave amplitudes as spatially uniform and consider the development of the scattering in time only. The entire analysis may be generalized to a weakly inhomogeneous plasma.[12,38]

We represent the electromagnetic waves, linearly polarized in the y direction and propagating in the $\pm x$ direction, by their transverse oscillation velocities,

$$u_y(x,t) = u_1(t)\exp(-i\omega_1 t + ik_1 x) + u_2(t)\exp(-i\omega_2 t - ik_2 x) + \text{c.c.}, \quad (1)$$

with slowly varying amplitudes u_1 and u_2 of the two opposed transverse waves ($\omega_1 > \omega_2$); the wavenumbers satisfy the dispersion relation $k^2c^2 = \omega^2 - \omega_p^2$, where ω_p is the unperturbed plasma frequency.

We cast the density perturbation in a beat representation

$$\delta n(x,t) = \sum_{\ell} \tilde{n}_\ell(t)\exp(-i\ell\Theta) + \text{c.c.} = \tilde{n}_1(t)\exp(-i\omega_0 t + ik_0 x) + \text{c.c.} + \ldots \quad (2)$$

where $\Theta \equiv \omega_0 t - k_0 x$, $\omega_0 = \omega_1 - \omega_2$ is the beat frequency, and $k_0 \equiv k_1 + k_2$ is the beat wavenumber. (Henceforth, we shall drop the subscript on the amplitude of the fundamental.) The neglect of the density perturbations

at the sum frequencies ($\omega_1 + \omega_2$, $2\omega_1$, and $2\omega_2$) has been discussed in Reference 12.

We adopt a cold fluid model[5,12] for the transverse velocity; the current density is thus $j_y(x,t) = u_y(x,t)\left[n_0 + \delta n(x,t)\right]$. The density perturbation δn is not necessarily small compared to n_0, and its calculation will be fully kinetic. We follow Reference 12 and obtain from Maxwell's equations and the fluid dynamical equations

$$du_1/dt = -(i/2)\ (\omega_p^2/\omega_1)\ (\tilde{n}/n_0)\ u_2$$

$$du_2/dt = -(i/2)\ (\omega_p^2/\omega_2)\ (\tilde{n}^*/n_0)\ u_1, \qquad (3)$$

where only slow temporal variations are kept in the nonlinear coupling terms. We note on the right sides of Equations (3) that the coupling strength is independent of n_0, which cancels, and that $\tilde{n}$ may be arbitrarily large. Multiple scattering and the couplings to other transverse waves arising from the density perturbations at the harmonics of the beat frequency and beat wavenumber are ignored. We also neglect collisional damping throughout the analysis.

We introduce $\tilde{\phi}_0(t)$, the slowly varying (complex) amplitude of the ponderomotive potential,

$$\tilde{\phi}_0(t) = (m/e)u_1 u_2^*.$$

The electron charge is taken to be e. The ponderomotive force associated with this potential is just the beat-frequency component of the longitudinal $\vec{v} \times \vec{B}$ force on the electrons due to the high frequency waves. The amplitude of the ponderomotive field is given by $\tilde{E}_0(t) = -ik_0\tilde{\phi}_0(t)$. The ponderomotive force drives the density perturbations.

The wave-action density of each transverse wave is given[12] by $J = \omega(m/e)^2|u|^2/2\pi$, and the wave energy density is ωJ. The conservation law for transverse-wave-action density is obtained directly from Equation (3)

$$(d/dt)(J_1 + J_2) = 0. \tag{4a}$$

Use of the continuity equation,

$$-i\omega_0 e\tilde{n}(t) + ik_0\tilde{j}_x(t) = 0,$$

(where $\tilde{j}_x(t)$ is the slowly varying amplitude of the beat-wave current) yields the action transfer rate

$$dJ_1/dt = -2Re(\tilde{E}_0\tilde{j}_x^*)/\omega_0. \tag{4b}$$

We introduce the wave-amplitude phases θ defined by $u \equiv |u|\exp(-i\theta)$ and determine from Equation (3) the additional relation,

$$J\delta\omega = Re(e\tilde{n}^*\tilde{\phi}_0), \tag{5}$$

for $\delta\omega \equiv d\theta/dt$, the nonlinear frequency shift of each transverse wave. Equations (4) and (5) are valid for linear or nonlinear density perturbations, and can be generalized to the case of a nonuniform magnetized plasma and to the inclusion of the spatial dependences and convection of the transverse-wave amplitudes.[12]

Conservation of transverse-wave action density implies that transverse-wave energy and momentum densities, $W = \omega J$ and $\vec{P} = \vec{k}J$, are not conserved. Their (non-)conservation laws are deduced from Equation 4b;

$$\begin{aligned}(d/dt)(W_1 + W_2) &= \omega_1 dJ_1/dt + \omega_2 dJ_2/dt \\ &= (\omega_1 - \omega_2)dJ_1/dt \equiv \omega_0 dJ_1/dt = -2Re(\tilde{E}_0\tilde{j}_x^*)\end{aligned} \tag{6}$$

and

$$(d/dt)(\vec{P}_1 + \vec{P}_2) = -(\vec{k}_0/\omega_0)2\mathrm{Re}(\tilde{E}_0\tilde{j}_x^*). \qquad (7)$$

Equations (6) and (7) state that the rate of energy and momentum lost or gained by the transverse waves equals the rate at which energy and momentum are deposited into or withdrawn from the plasma by the ponderomotive force.

We deduce from Equations (4), (6), and (7) that the rate of action transfer, and hence of energy and momentum transfer, is zero when $\tilde{E}_0$ and $\tilde{j}_x$ (or $\tilde{n}$) are 90° out of phase. From Poisson's equation for the self-consistent potential, $\phi(x,t) = \sum_\ell \tilde{\phi}_\ell(t)\exp(-i\ell\Theta) + \text{c.c.} = \tilde{\phi}(t)\exp(-i\Theta) + \text{c.c.} + \ldots$, we obtain $\tilde{\phi} = 4\pi\tilde{n}e/k_0^2$ and conclude that there is no action transfer when $\tilde{\phi}$ and $\tilde{\phi}_0$ have a relative phase of 0° or 180°. There is then no momentum transfer nor work done by the ponderomotive force, and the transverse waves acquire steady nonlinear frequency shifts as the consequence of the coupling: $\delta\omega = J^{-1}\mathrm{Re}(e\tilde{n}^*\tilde{\phi}_0)$. Any eventual steady state must be consistent with these conditions and relations.

We have shown elsewhere[15] that the (possibly nonlinear) dielectric response to the ponderomotive potential can be expressed as $\tilde{\phi}(t) = \left[\varepsilon^{-1}(k_0,\omega_0 + id_t) - 1\right]\tilde{\phi}_0(t)$. We describe the plasma response to be "quasi-steady" when we can set $d/dt = 0$ in evaluating the dielectric function, i.e., $\varepsilon(k_0,\omega_0 + id_t)\left[\tilde{\phi}(t) + \tilde{\phi}_0(t)\right] \to \varepsilon(k_0,\omega_0)\left[\tilde{\phi} + \tilde{\phi}_0\right]$. Use of the Poisson equation and the quasi-steady limit of the dielectric function in Equations (4) and (5) gives

$$dJ_1/dt = -dJ_2/dt = \mathrm{Im}(\varepsilon^{-1})|\tilde{E}_0|^2/2\pi \qquad (8)$$

and

$$d\omega J = \mathrm{Re}(\varepsilon^{-1} - 1)|\tilde{E}_0|^2/4\pi \qquad (9)$$

In the quasi-steady limit, the nonlinear dielectric function, evaluated near a resonance, is given approximately by

$$\epsilon(k_0,\omega_0) \approx \bar{\epsilon}(\omega_{n\ell})\left[\omega_0 - \omega_{n\ell}\right] \equiv \bar{\epsilon}(\omega_{n\ell})\left[\Delta + i\nu\right], \tag{10}$$

where the nonlinear eigenfrequency $\omega_{n\ell}$, satisfies $\epsilon(k_0,\omega_{n\ell}) = 0$, and $\bar{\epsilon} \equiv \partial\epsilon/\partial\omega$. The frequency mismatch Δ and the dissipation rate ν are defined by $\Delta \equiv \omega_0 - \mathrm{Re}\ \omega_{n\ell}$ and $\nu \equiv -\mathrm{Im}\,\omega_{n\ell}$. For weakly nonlinear waves, $\bar{\epsilon}(\omega_{n\ell}) \approx 2\omega_p^{-1}$ if $k_0\lambda_e \ll 1$, where $\lambda_e \equiv v_e/\omega_p$ is the electron Debye length. The justification of the quasi-steady approximation in Equation (10) requires that $|\omega_0 - \omega_{n\ell}| \gg |d/dt|$.

We can use Equation (10) to express the right sides of Equations (8) and (9) as $-(\nu\omega_p/2\Delta^2)|\tilde{E}_0|^2/2\pi$ and $(\omega_p/2\Delta)|\tilde{E}_0|^2/4\pi$, respectively, for $|\nu| \ll |\Delta| \ll \omega_p$. It is evident that irreversible action, energy, and momentum transfer require finite dissipation in the plasma dielectric response. The reversible action transfer that three coupled linear normal modes exhibit (described by Sagdeev and Galeev[27]) does not occur here, because of heavy damping. However, if the dissipation of the density perturbation oscillates about zero, because of the bouncing of trapped particles, for example, the action transfer will also oscillate. Only if the dissipation asymptotically were to vanish, and the frequency shift to approach a finite value would action transfer cease. The transverse waves would then exhibit constant nonlinear frequency shifts also [Equations (5) and (9)].

We define the total response potential Φ as the sum of the Coulomb ϕ and ponderomotive ϕ_0 potentials:

$$\Phi(x,t) \equiv \phi(x,t) + \phi_0(x,t) \equiv \tilde{\Phi}(t)\exp(-i\omega_0 t + ik_0 x) + c.c. + \ldots$$

In References 15 and 38 we have demonstrated that the time-dependent complex eigenfrequency $\omega_{n\ell}$ can be constructed from a knowledge of $\tilde{\Phi}(t)$ and $\tilde{\phi}_0(t)$ by utilizing a Taylor series expansion of the nonlinear dielectric function. To lowest order in $|\omega_0 - \omega_{n\ell} + i(d/dt)|/|\omega_{n\ell}| << 1$, we have obtained

$$\left[\omega_0 - \omega_{n\ell} + i(d/dt)\right]\tilde{\Phi}(t) = \tilde{\phi}_0(t)/\bar{\varepsilon}(\omega_{n\ell}). \tag{11}$$

The nonlinear frequency shift $\delta\Omega \equiv \mathrm{Re}(\omega_{n\ell} - \omega_\ell)$ [the linear eigenfrequency ω_ℓ is determined from the linear dielectric function: $\varepsilon_\ell(\omega_\ell, k_0) = 0$] and the nonlinear dissipation $\nu \equiv \mathrm{Im}\,\omega_{n\ell}$ are deduced[15] from the simulation results, using Equation (11) with $\bar{\varepsilon}(\omega_{n\ell}) \approx 2\omega_p^{-1}$. Only for weakly nonlinear, freely propagating plasma waves, has perturbation theory been successfully used to analytically construct $\varepsilon_{n\ell}$ and $\omega_{n\ell}$, when to good approximation the wave amplitude could be assumed constant in calculating the perturbed particle orbits.[41] The phenomenon considered here is dominantly nonlinear and demands a fully self-consistent, non-perturbative description. This encourages the use of particle simulation, a discussion of which follows in the next section.

To further emphasize the degree of nonlinearity in the phenomena considered here, we formally integrate Equation (11):

$$\tilde{\Phi}(t) = -i\int_0^t dt'\bar{\varepsilon}(t')^{-1}\tilde{\phi}_0(t')\exp\left[i\int_{t'}^t dt''\Delta_{n\ell}(t'')\right], \tag{12}$$

where $\Delta_{n\ell} \equiv \omega_0 - \omega_{n\ell}$. The plasma response is secular near the resonance $\Delta_{n\ell} \approx 0$; however, the interaction of the beat-wave potential $\phi_0(x,t)$ with the plasma is shifted away from resonance by the nonlinear electron

dynamics. There is induced a finite, complex-valued $\Delta_{n\ell}$. Equation (12) describes the ensuing modulation of the total potential $\tilde{\Phi}(t)$ at the mismatch frequency $\Delta_{n\ell}$. There is modulation also at the bounce frequency, if there is trapping.[15,41] When the nonlinear frequency shift or dissipation becomes appreciable in magnitude compared to the plasma frequency ω_p, the Taylor-series expansion leading to Equation (11) is no longer valid.

When the three-wave decay becomes nonresonant we must re-examine the neglect of the density perturbations at the frequencies $2\omega_1$, $2\omega_2$, and $\omega_1 + \omega_2$ as compared to the low frequency-beat perturbation. The former perturbations have high phase velocities for which there are few resonant particles. Consequently, Im $\varepsilon \approx 0$ and Re $\varepsilon \approx 1$; the plasma response is essentially reactive. As these density perturbations contribute to the nonlinear transverse current, there are additional nonlinear couplings which are additive to the right sides of Equations (3-9). However, because the plasma response is reactive, these couplings only induce small frequency shifts in the transverse waves.[12] These shifts scale as $|u/c|^2$ and are therefore the same order as relativistic effects[49] which have been ignored throughout. This justifies the continued neglect of the high frequency density perturbations.

On the other hand, the low frequency beat-wave can continue to interact with the plasma in an interesting and significant fashion, even when electron plasma waves are no longer resonantly excited. A wave-particle resonance remains accessible to the beat-wave: $\omega_1 - \omega_2 = (\vec{k}_1 - \vec{k}_2)\cdot\vec{v}$. When this resonance condition is satisfied by a large number of electrons and the distribution function has finite slope at the resonant velocity,

stimulated Thomson scattering occurs.[5,16-19] Im ε is then appreciable, and the plasma response is considerably resistive. In fact, the beat-wave can be heavily damped, with action transfer continuing nevertheless. Therefore, in our simulations we have followed the temporal development of the scattering well into regimes in which the beat-wave is heavily damped.

IV. Computer Simulations

Numerical simulations were performed to investigate the back-reaction of trapping on the scattering of the transverse waves in a regime of non-linearity where analytical perturbation theory fails. This regime[41] corresponds to $v_t\omega_0/k_0 \geq v_e^2$, where the trapping velocity v_t is defined as $v_t \equiv |2e\tilde{\Phi}/m|^{1/2}$ and $v_e \equiv (T/m)^{1/2}$. The simulation plasma was taken to be periodic and initially uniform. The equations for the transverse-wave amplitudes, Equations (3), were adjoined to a one dimensional, electrostatic particle code[44] (ES1); integrations were performed forward in time, treating the stimulated scattering as a time-dependent initial value problem. At each time-step, the transverse wave amplitudes were incrementally changed according to Equation (3), using a first-order Euler differencing scheme. The ponderomotive potential $\phi_0(x,t)$ was then constructed, and the electron velocities and positions advanced using the gradient of the ponderomotive and self-consistent Coulomb potentials. Ions were treated as a fixed charge-neutralizing background. The self-consistent Coulomb potential was obtained from solution of Poisson's equation given the charge density. Finally, from the Fourier component of the density perturbation, at the beat wavenumber and frequency, the coupling of the transverse waves was calculated using Equation (3).

By adjoining the coupled mode equations to an electrostatic simulation, there is then no restriction on the time-step of the integration due to the high frequency waves, which would otherwise require that $\omega_1\Delta t << 1$ in addition to $\omega_p\Delta t << 1$. In practice, the time step satisfied $\omega_p\Delta t \leq 0.2$. Energy, momentum and action were all conserved within a few percent.

This simulation scheme precludes the possibility of the two transverse waves scattering further into any other electromagnetic waves.[32] Immobilizing the ions prevents interactions of the transverse waves and the excited plasma wave with the ions, for example, the parametric decay of the electron plasma wave into another plasma wave and an ion acoustic wave.[50] Reference 38 describes the range of parameters for which electron trapping can occur well before parametric instabilities involving ions are significant.

In our simulations, we chose the following parameters:

$$\omega_0 = \omega_p,\ \omega_1 = 5\omega_p,\ \omega_2 = 4\omega_p,\ u_1(0) = u_2(0), \text{ and } \omega_0/k_0 = 3v_e = c/9.$$

This choice of beat-wave phase velocity relative to the electron thermal velocity causes the resonantly excited plasma wave to be weakly damped according to linear theory. However, with $\omega_0/k_0 = 3v_e$ there is a reasonable number of simulation particles at $v \approx \omega_0/k_0$ even with only a modest total number (4000) of simulation particles. The range of transverse wave amplitudes considered was $0.3 \leq |u_1(0)/v_e| \leq 0.9$, which induced ponderomotive potentials of magnitude $0.09 \leq |e\tilde{\phi}_0/T| \leq 0.9$.

Results typical of simulations exhibiting considerable trapping are shown in Figures 1-5. The (total) electric field response $E = -(\partial/\partial x)\Phi(x,t)$,

longitudinal phase space, and the longitudinal velocity distribution function are displayed in Figure 1 at $\omega_p t/2\pi$ = 6, 68, and 125. At early times there is a large amplitude response driven nearly in phase with the ponderomotive force (Figure 1a); longitudinal phase space has a hole centered over the bottom of the potential well (Figure 1b); and the distribution function has a distended, nonmaxwellian tail for $v \geq \omega_0/k_0$ (Figure 1c). At later times the electric field response and the ponderomotive force are both weaker than at early times and out of phase. The total potential well is not so deep as before, and the hole in phase space (related to the separatrix between trapped and untrapped electrons) is reduced. The distribution function is further deformed concomitant with the continued scattering.

In Figures 2a and 2b are plotted the (real) amplitudes of the ponderomotive potential and response, and their respective phases, as functions of time. The plasma response builds rapidly to a relatively large amplitude in a few plasma periods. Initially the phase of the response relative to the ponderomotive potential is $\pi/2$, which is the appropriate phase for a maximum rate of action transfer out of the high frequency transverse wave. Later in time, as a consequence of nonlinear effects, the response amplitude and phase are modulated dominantly on the time scale of the mismatch $|\omega_0 - \omega_{n\ell}| \leq 0.1\omega_p$ as described by Equation (12). In addition, the response amplitude has superimposed a finer scale, more rapid oscillation at the directly observed bounce frequency of trapped electrons $\omega_t^o \sim 0.5\ \omega_p$. (The phase-space trajectories of individual electrons were followed in the rest frame of the beat wave.) This bounce frequency is slightly less than

the standard bounce frequency of a deeply trapped particle $\omega_t^s \equiv k_0 v_t$, which is calculated from the time-averaged amplitude of $\Phi(x,t)$. The tendency for $\omega_t^o < \omega_t^s$ was observed and discussed in Reference 15, and is consistent with particles not being trapped near the bottom of the potential well, for which the hole in longitudinal phase space is good evidence (Figure 1b). Because $|\omega_0 - \omega_{n\ell}| << \omega_t^o, \omega_t^s$ there can exist trapped particles which respond more or less adiabatically to the modulation of the potential produced by the mismatch. However, particles near the separatrix do not respond adiabatically and are observed to suffer recurrent trapping and detrapping.

The ponderomotive potential, as well as the response, oscillates on the mismatch and trapping time scales, due to the reaction of the density perturbation back on the coupling of the transverse waves according to Equation (4). However, the oscillations of $\tilde{\phi}_0(t)$ are of lesser degree than for $\tilde{\Phi}(t)$. The general decrease of $|\tilde{\phi}_0|$ is due to depletion of the high frequency transverse wave. After the early period of considerable action transfer and strong plasma response, the relative phase $\theta - \theta_0$ oscillates fairly steadily but with large excursion ($\pm \pi/2$) around zero with frequency approximately equal to the mismatch $\Delta_{n\ell}(t)$. One recalls from Equation (4) that a relative phase of zero corresponds to no action transfer, and $\pm\pi/2$ corresponds to relative extrema of the action transfer rate for fixed $|\tilde{E}_0|$ and $|\tilde{j}_x|$.

In Figure 3 are shown the nonlinear frequency shift $\delta\Omega$ and the total dissipation rate ν as deduced using Equation (11). Initially the damping rate far exceeds the linear Landau damping rate, $\nu_\ell/\omega_p = 0.03$. In the small amplitude limit, only resonant particles ($v \sim \omega_0/k_0$) contribute to

the damping of the wave. However, when the wave amplitude is finite, the resonance width is broadened. The nonlinear damping can be quite large depending on how much of the velocity distribution function is resonant and the relative preponderance of resonant particles with velocities $v < \omega_0/k_0$. This phenomenon has been observed in experiments and simulations, and understood theoretically.[51] As our simulation progresses the dissipation exhibits fairly large oscillations around zero at the mismatch frequency and smaller, more rapid variations at the trapping frequency ω_t^o. The frequency shift also exhibits modulation effects and is negative in keeping with the presence of trapped particles.[41] A detailed discussion of the time dependence of the deduced frequency shift and dissipation rate, and its relation to the modulation and trapped-particle effects, is contained in Reference 15.

Later in the simulation, we observe a general increase of the mismatch $|\omega_0 - \omega_{n\ell}|$, and hence decrease of $|\tilde{\Phi}/\tilde{\phi}_0|$. This is closely related to the continued deformation of the velocity distribution function as implied by momentum and energy conservation laws, Equations (3) and (4) of Reference 15. The conservation laws illustrate the dependences of the nonlinear dissipation on the momenta of the resonant electrons, and of the nonlinear frequency shift on their kinetic energy. The deduced frequency shift and dissipation are not shown past $\omega_p t/2\pi = 25$ in Figure 3 because of the breakdown of the expansion procedure leading to Equation (11) when the (complex-valued) frequency mismatch is large. At this point, the electron plasma wave ceases to be resonantly excited; but action transfer continues as a nonlinear form of induced Thomson scattering. Many particles satisfy the condition

$\omega_1 - \omega_2 \approx (\vec{k}_1 - \vec{k}_2)\cdot\vec{v}$, i.e., $\omega_0 \approx k_0 v$, and have orbits which have been strongly perturbed. Over a trapping region $v = (\omega_0/k_0) \pm v_t$, the distribution function has finite, time-dependent slope (see Figure 1c). Late in time, when not much action is transferred on average, the sign of the slope and the direction of action transfer oscillate.[18,19]

In Figure 4 appear the amplitudes and phases of the three interacting waves u_1, u_2, and $\tilde{n}$ as functions of time. As described earlier, the amplitude of the density perturbation oscillates principally at the mismatch frequency and also at the trapping frequency ω_t^o. It decreases in magnitude due to dissipation, the increase of $|\Delta_{n\ell}|$ and the decrease of the ponderomotive potential. The phase of the density perturbation seems to be modulated at the mismatch frequency and not significantly[15] at ω_t^o. The slowly varying wave phase θ_2 is fairly constant over the duration of the simulation, but θ_1 is significantly modulated at the frequency $\mathrm{Re}\Delta_{n\ell}$ once there is much less wave action associated with it [see Equations (5) and (9)].

The energy of the higher frequency transverse wave depletes by approximately 90%, and the energy transfer is essentially complete after fifteen Langmuir oscillation periods ($\omega_p t/ 2\pi = 15$). Although the action transfer is rapid, it nevertheless occurs over many trapped-particle bounce periods, viz. eight periods ($\omega_t^o t/2\pi \sim 8$). Hence, the stimulated scattering does not immediately terminate with the onset of trapping.[13,14] On the bounce time scale, the amplitudes $|u_1|$ and $|u_2|$ have slight variations in accordance with Equations (4) and (8).

The relative energy transfer (from the ω_1-wave) to plasma oscillations and longitudinal kinetic energy is given by $0.9\ (\omega_0/\omega_1) = 0.9\ (1/5) = 0.18$. This 18% of the higher frequency transverse-wave energy deposited in the plasma results in a five-fold increase of the plasma thermal energy relative to its initial value. Very little energy ends up in a coherent oscillation (BGK wave). The action transfer $\Delta J/J_1(0) \approx 0.9$ also accounts for a relative momentum transfer to the plasma $k_0\Delta J/k_1 J_1(0) \approx 1.8$, and the plasma acquires a longitudinal drift velocity equal to $1.2\ v_e(0)$.

The spatically averaged longitudinal kinetic and electric field energy densities are displayed in Figure 5 as functions of time up to $\omega_p t/2\pi = 40$. Accompanying the excitation of the large amplitude electron plasma wave and transfer of action early in the simulation is a large increase in plasma kinetic energy, which soon exceeds the field energy by more than an order of magnitude. Although there is significant damping of the longitudinal field energy, it remains well above the thermal fluctuation level. [For our one-dimensional simulation plasma, the fluctuation level is reduced by the use of finite-sized particles to a value which is given initially by $\langle(\partial\phi/\partial x)^2/8\pi\rangle < (N\lambda_e/L)^{-1} n_0 T(0)/2 \approx 0.25 \times 10^{-2} n_0 T(0)$, where N is the number of simulation particles (4000) and $\lambda_e/L \approx 0.05$ is the ratio of the initial Debye length to the length of the plasma]. For later times not shown in Figure 5, the field energy density continues to slowly decrease and the kinetic energy very slightly increases. Both continue to exhibit some modulation.

The disparity between the longitudinal field energy and the kinetic energy demonstrates that the ponderomotive force of the transverse waves

deposits most of the available energy into the plasma and not into long-lived plasma waves. The mechanism for this is furnished by the early onset of trapping and the associated damping with a rate in excess of the linear rate. One might have expected a significant fraction of the energy to end up in a large amplitude BGK wave. This would seem especially likely in the case studied here, because our choice of the fundamental wavelength of the simulation for the beat-wave has precluded the sideband instability, a favorite mechanism for the break-up of BGK waves.[52] Nevertheless, there is no evidence of a BGK wave late in time in our simulations.

In other simulations different values of the initial transverse wave amplitudes or frequencies were chosen. Large wave amplitudes tended to shorten the time scales for the onset of nonlinear effects without qualitatively altering the physical phenomena. By altering the choice of the wave frequencies, the linear mismatch frequency $\omega_0 - \omega_\ell$ was varied. For weaker transverse wave amplitudes the nonlinear phenomena were more sensitive to the linear mismatch, i.e. trapping and efficient energy/momentum transfer to the plasma demanded smaller mismatch frequencies for smaller $|u_1|$ and $|u_2|$ so that stimulated Raman scattering would be more nearly resonant. On the other hand, for larger values of $|u_1|$ and $|u_2|$ trapping effects and the rate and amount of irreversible action transfer were less sensitive to the linear mismatch.

We have observed, both here and in the simulations described in Reference 15, the approximate constancy in time of the observed trapping frequency ω_t^o, despite the significant modulation of and the general decrease in the amplitude of the plasma wave. This has also been observed in many

simulations and experiments in which the propagation of a single large amplitude electron plasma wave has been studied.[53] A decrease in the depth of the potential well ought to reduce the trapping frequency, $\omega_t^s \propto |\tilde{\phi}|^{1/2}$. In our simulations this seems to be counterbalanced by the falling of the trapped electrons toward the bottom of the potential well, which is evidenced by the filling in of the hole in phase space (Figure 1c).

IV. Summary

Our simulations of Raman scattering have exhibited extensive electron trapping and deformation of the velocity distribution function, relatively large nonlinear frequency shifts and dissipation, considerable energy and momentum transfer, and a transition to induced Thomson scattering. By use of coupled-mode equations for the electromagnetic waves and a ponderomotive potential to describe their nonlinear interaction, together with a standard one-dimensional electrostatic particle code, economically efficient and conceptually simple simulations were performed on the electron plasma wave time scale.

Various nonlinear effects due to electron trapping were observed and interpreted self-consistently in the longitudinal field response, the nonlinear frequency shift and dissipation, and the reaction of the density perturbation back on the coupled transverse waves. The simulations have demonstrated the application of a prescription for analyzing the nonlinear dielectric response proposed in Reference 15, which we have found useful in understanding the self-consistent interplay of the nonlinear effects.

We have derived general relations, Equations (4) and (5), describing stimulated Raman and Thomson scattering in terms of wave-action transfer

and nonlinear frequency shifts. We have found in simulation that an electron plasma wave can be resonantly excited to large amplitude and then can nonlinearly shift its normal mode frequency. The interaction of the transverse waves with the plasma wave is thus shifted away from resonance. The ponderomotive beat-wave can directly resonate with particles, and much of the energy in the higher frequency transverse wave can thus be rapidly depleted. We conclude from our computer simulations that the plasma can absorb most of the available energy as kinetic energy with only a small fraction residing in the longitudinal electric field. The lower frequency transverse wave is amplified consistent with the conservation of transverse-wave action.

Our simulations thus support the contention that the ultimate efficiency of plasma beat-heating and plasma-laser amplification is limited only by the Manley-Rowe relation. Hence, our present results concerning the effects of electron trapping on stimulated Raman and Thomson scattering are encouraging for these practical applications. However, the continued stimulated backscattering of laser light after the onset of trapping may be discouraging for laser-fusion.

Acknowledgments

We are greatly indebted to Drs. A. B. Langdon and C. K. Birdsall for furnishing the original computer code ES1 and for their continued encouragement and interest, and to Dr. G. Smith for assisting with code modifications. We also thank Drs. S. Johnston, G. Morales, M. Mostrom, D. Nicholson, T. O'Neil, and F. Perkins for many useful discussions.

This work was supported by the U.S. Energy Research and Development Administration.

References

[1]C. V. Raman and U. S. Krishan, Nature 121, 501 (1928).

[2]Y. R. Shen and N. Bloembergen, Phys. Rev. 137, 1787 (1965).

[3]N. Bloembergen, Am. J. Phys. 35, 989 (1967).

[4]Y. R. Shen, Rev. Mod. Physics 48, 1 (1976).

[5]J. F. Drake, P. K. Kaw, Y. C. Lee, G. Schmidt, C. S. Liu, and M. N. Rosenbluth, Phys. Fluids 17, 778 (1974).

[6]N. M. Kroll, A. Ron, and N. Rostoker, Phys. Rev. Letters 13, 85 (1964).

[7]B. I. Cohen, A. N. Kaufman, and K. M. Watson, Phys. Rev. Letters 29, 581 (1972).

[8]M. N. Rosenbluth and C. S. Liu, Phys. Rev. Lett. 29, 701 (1972).

[9]A. N. Kaufman and B. I. Cohen, Phys. Rev. Lett. 30, 1306 (1973).

[10]V. Fuchs, C. Neufeld, J. Teichman, and A. G. Ehgelhardt, Phys. Rev. Lett. 31, 1110 (1973).

[11]B. I. Cohen, Phys. Fluids 17, 496 (1974).

[12]B. I. Cohen, M. A. Mostrom, D. R. Nicholson, A. N. Kaufman, C. E. Max, and A. B. Langdon, Phys. Fluids 18, 470 (1975).

[13]D. W. Forslund, J. M. Kindel, and E. L. Lindman, Phys. Fluids 18, 1002 (1975); and Phys. Fluids 18, 1017 (1975).

[14]H. H. Klein, E. Ott, and W. M. Manheimer, Phys. Fluids 18, 1031 (1975).

[15]B. I. Cohen and A. N. Kaufman, Phys. Fluids 20, 1113 (1977).

[16]A. G. Litvak and V. Yu Trakhtengerts, Zh. Eksp. Teor. Fiz. 60, 1702 (1971) [Sov. Phys.—JETP 33, 921 (1971)].

[17]A. G. Litvak, V. Petrukhina, and V. Yu Trakhtengerts, Zh. Eksp. Teor. Fiz. Pis. Red. 18, 190 (1973) [Sov. Phys—JETP Letters 18, 111 (1973)].

[18]R. S. Johnston, Phys. Fluids 19, 93 (1976).

[19]R. S. Johnston and R. M. Kulsrud, Phys. Fluids 20, 829 (1977).

[20]L. Brillouin, Ann. Physics (Paris) 17, 88 (1922).

[21]Advances in Plasma Physics, edited by A. Simon and W. B. Thompson (Wiley, New York, 1976), Vol. 6, Pt. 1.

[22]W. H. Louisell, Coupled Mode and Parametric Electronics (Wiley, New York, 1960).

[23]J. Dougherty, J. Plasma Phys. 4, 761 (1970).

[24]J. Galloway and H. Kim, J. Plasma Phys. 6, 53 (1971).

[25]L. Altshul and V. Karpman, Zh. Eksp. Teor. Fiz. 47, 1544 (1964). [Sov. Phys—JETP 20, 1043 (1965)].

[26]D. Melrose, Plasma Phys. 14, 1035 (1972).

[27]R. Z. Sagdeev and A. A. Galeev, Nonlinear Plasma Theory (Benjamin, New York, 1969).

[28]V. E. Zakharov and S. V. Manakov, Zh. Eksp. Teor. Fiz. 69, 1654 (1975) [Sov. Phys.—JETP 42, 842 (1976)].

[29]A. H. Reiman, A. Bers, and D. J. Kaup, Phys. Rev. Letters 39, 245 (1977).

[30]C. L. Tang, J. Appl. Physics 37, 2945 (1966).

[31]K. H. Spatschek, M. Y. Yu, and P. K. Shukla, Plasma Physics 18, 573 (1976); F. Y. F. Chu and C. F. F. Karney, "Solution of the Three-Wave Resonant Equations with One Wave Heavily Damped" (submitted to Phys. Fluids).

[32]A. T. Lin and J. M. Dawson, Phys. Fluids 18, 201 (1975).

[33]C. R. James and W. B. Thompson, Can. J. Phys. 45, 1771 (1967).

[34]C. E. Capjack and C. R. James, Can. J. Phys. 48, 1386 (1970).

[35]G. Weyl, Phys. Fluids 13, 1802 (1970).

[36]B. Stansfield, R. Nodwell, and J. Meyer, Phys. Rev. Letters 26, 1219 (1971).

[37]G. Schmidt, Phys. Fluids 16, 1676 (1973).

[38]B. I. Cohen, Ph.D. thesis, University of California (1975). (University Microfilms, Ann Arbor, 76-15144).

[39]R. C. Davidson, Methods in Nonlinear Plasma Theory (Academic Press, New York, 1972), Part I.

[40]B. B. Kadomtsev and V. I. Karpman, Usp. Fiz. Nauk 103, 193 (1971) [Sov. Phys.-Usp. 14, 40 (1971)].

[41]G. J. Morales and T. M. O'Neil, Phys. Rev. Letters 28, 417 (1972).

[42]K. Nishikawa, H. Hojo, K. Mima, and H. Ikezi, Phys. Rev. Letters 33, 148 (1974).

[43]D. L. Book and P. A. Sprangle, Bull. Phys. Soc. 19, 882 (1974); J. P. Boris and D. L. Book in Methods of Computational Physics, edited by J. Killeen (Academic, New York, 1976), Vol. 16, p. 123.

[44]C. K. Birdsall and A. B. Langdon, Plasma Physics via Computer Simulation (to be published).

[45]R. D. Milroy, C. E. Capjack, and C. R. James (to be published in Plasma Physics).

[46]W. M. Manheimer and E. Ott, Physical Fluids 17, 463 (1974).

[47]P. A. Sprangle and V. L. Granatstein, Appl. Phys. Letters 25, 377 (1974).

[48]T. Kwan, J. M. Dawson, and A. T. Lin, Phys. Fluids 20, 581 (1977).

[49]J. Arons and C. E. Max, Phys. Fluids 17, 1983 (1974).

[50]M. V. Goldman and D. F. DuBois, Ann. Phys. (N.Y.) 38, 117 (1966); K. Nishikawa, J. Phys. Soc. Japan 24, 916 (1968), V. P. Silin, Zh. Eksp. Teor. Fiz. 48, 1679 (1965) [Sov. Phys.—JETP 21, 112 (1965)].

[51]J. M. Dawson and R. Shanny, Phys. Fluids 11, 1506 (1968); R. Sugihara and K. Yamanaka, Phys. Fluids 18, 114 (1975); J. Canosa, Phys. Fluids 19, 1952 (1976).

[52]W. L. Kruer, J. M. Dawson, and R. N. Sudan, Phys. Rev. Letters 23, 838 (1969); W. L. Kruer and J. M. Dawson, Phys. Fluids 13, 2747 (1970).

[53]R. N. Franklin, S. M. Hamberger, and G. J. Smith, Phys. Rev. Letters 29, 914 (1972); H. Sugai and E. Mark, Phys. Rev. Letters 34, 127 (1975); G. Dimonte and J. H. Malmberg, Phys. Rev. Letters 38, 401 (1977).

Figure Captions

Figure 1. Simulation of the resonant response of a maxwellian electron plasma [thermal speed $v_e = (T/m)^{1/2}$] to a ponderomotive plane-wave driving force, of frequency ω_0 (chosen equal to ω_p) and phase velocity ω_0/k_0 (chosen equal to $3v_e$), induced by the $\vec{v} \times \vec{B}$ coupling of two opposed electromagnetic waves with oscillation velocity amplitudes u_1 and u_2 (chosen initially equal to $0.2\ \omega_0/k_0 = 0.6\ v_e$). Initially the linear normal mode frequency is $\text{Re}\ \omega_\ell = 1.17\ \omega_p$, and the linear Landau damping rate is $-\text{Im}\ \omega_\ell = 0.03\ \omega_p$. The transverse waves have frequencies $\omega_1 = 5\omega_p$ and $\omega_2 \equiv \omega_1 - \omega_0 = 4\omega_p$. For a typical simulation, we exhibit at $\omega_p t/2\pi =$ 6, 68, and 125 the following:

(a) the longitudinal driving field $E_0 = -\partial\phi_0/\partial x$ and the total longitudinal field $E = -\partial\Phi/\partial x$ as functions of x, in natural units;

(b) the longitudinal electron phase space;

(c) the longitudinal velocity distribution, with different scales and arbitrary units.

Figure 2. For the simulation in Figure 1, shown as functions of time are

(a) the magnitudes of the total and ponderomotive potentials in natural units, $e\Phi/(mv_\phi^2)$ and $e\phi_0/(mv_\phi^2)$ where $v_\phi \equiv \omega_0/k_0$,

(b) their respective phases θ and θ_0, defined by

$\Phi(x,t) = \Phi(t) \cos(\omega_0 t - k_0 x + \theta)$ and $\phi_0(x,t) = \phi_0(t) \cos(\omega_0 t - k_0 x + \theta_0)$.

Figure 3. For the simulation in Figure 1, shown schematically as functions of time (up to $\omega_p t/2\pi = 25$) are

(a) the deduced nonlinear frequency shift $\delta\Omega = \mathrm{Re}(\omega_{n\ell} - \omega_\ell)$, with the linear mismatch $\Delta_\ell \equiv \omega_0 - \omega_\ell$ indicated for reference;

(b) the nonlinear dissipation rate $\nu = -\mathrm{Im}\ \omega_{n\ell}$.

Figure 4. For the simulation in Figure 1, shown as functions of time are

(a) the magnitudes of the coupled-mode amplitudes $|u_1|/v_\phi$, $|u_2|/v_\phi$, and $|\tilde{n}|/n_0$ where $v_\phi \equiv \omega_0/k_0$;

(b) their respective phases θ_1, θ_2, and θ_n.

Figure 5. The spatially averaged longitudinal kinetic and field energy densities, $\langle nmv_x^2/2\rangle$ and $\langle(\partial\phi/\partial x)^2/8\pi\rangle$, vs. time (up to $\omega_p t/2\pi = 40$) for the simulation shown in Figure 1. The initial thermal fluctuation level for $\langle(\partial\phi/\partial x)^2/8\pi\rangle$ is less than $0.25 \times 10^{-2}\ n_0 T(0)$.

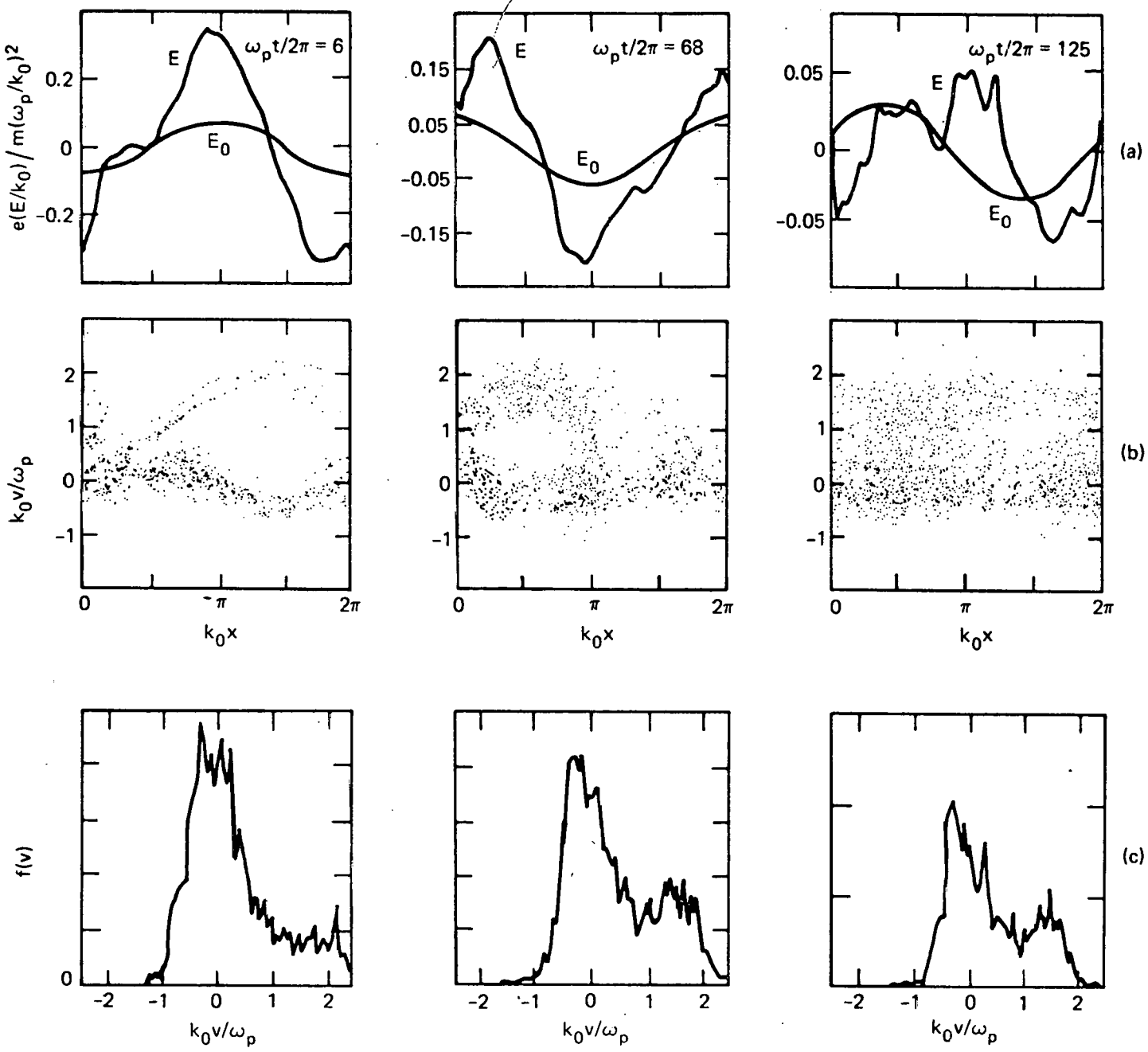
$e(E/k_0)/m(\omega_p/k_0)^2$
E
E_0
$\omega_p t/2\pi = 6$
$\omega_p t/2\pi = 68$
$\omega_p t/2\pi = 125$
0.2
0
-0.2
0.15
0.05
-0.05
-0.15
(a)
$k_0 v/\omega_p$
2
1
0
-1
π
2π
$k_0 x$
(b)
f(v)
-2
-1
0
1
2
$k_0 v/\omega_p$
(c)

Figure 1

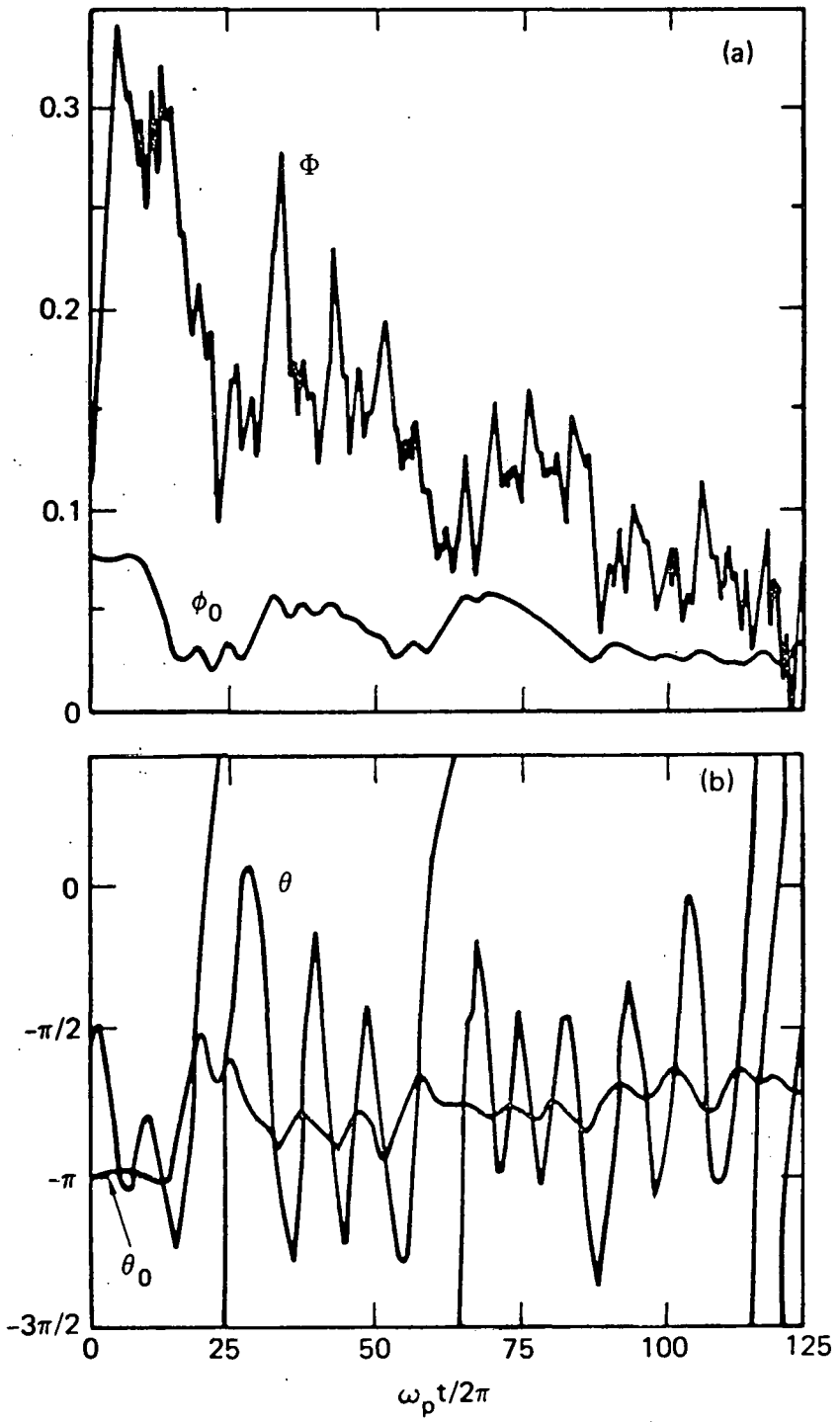
(a)
0.3
0.2
0.1
0
Φ
ϕ_0
(b)
0
-π/2
-π
-3π/2
θ
θ_0
0
25
50
75
100
125
$\omega_p t/2\pi$

Figure 2

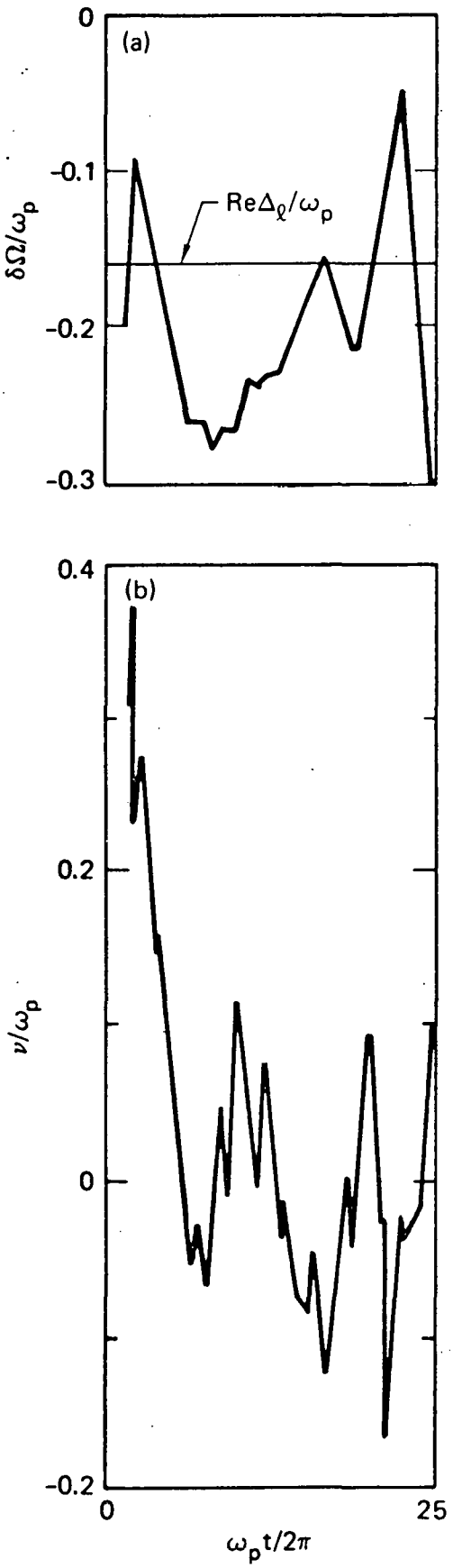
(a)
0
-0.1
-0.2
-0.3
$\delta\Omega/\omega_p$
$\mathrm{Re}\Delta_\ell/\omega_p$
(b)
0.4
0.2
0
-0.2
ν/ω_p
0
25
$\omega_p t/2\pi$

Figure 3

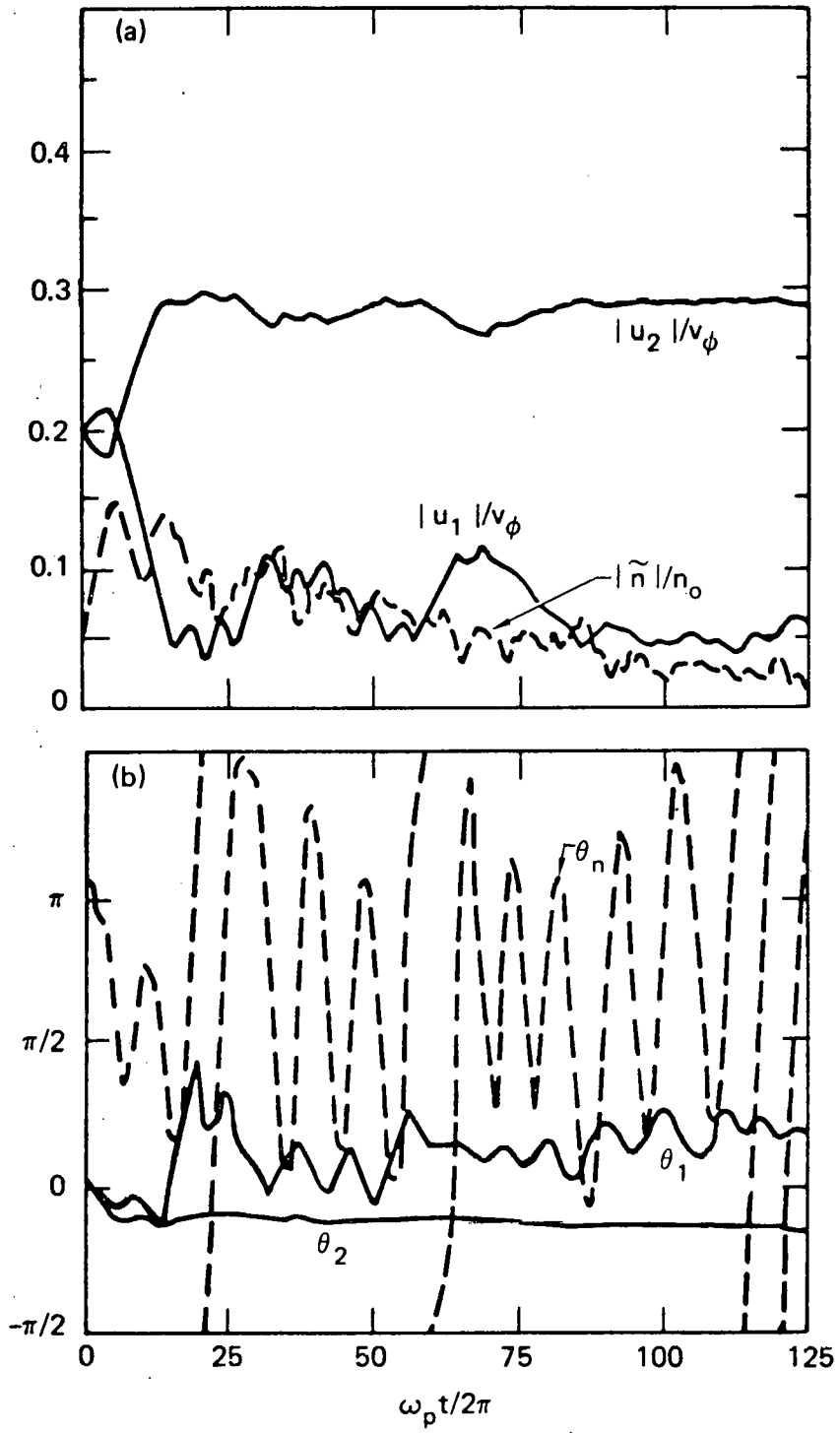
(a)
0.4
0.3
0.2
0.1
0
$|u_2|/v_\phi$
$|u_1|/v_\phi$
$|\tilde{n}|/n_o$
(b)
π
$\pi/2$
0
$-\pi/2$
θ_n
θ_1
θ_2
0
25
50
75
100
125
$\omega_p t/2\pi$

Figure 4

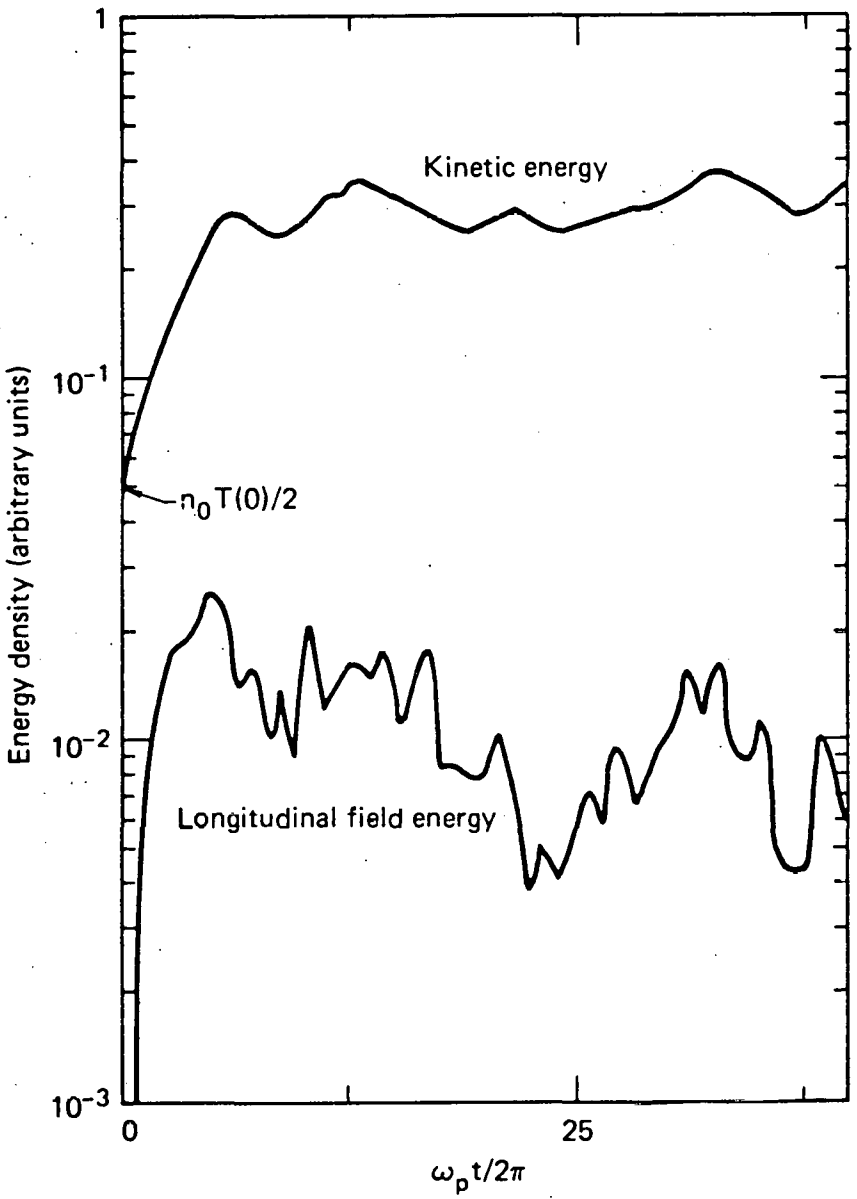
1
10^{-1}
10^{-2}
10^{-3}
Energy density (arbitrary units)
Kinetic energy
$n_0T(0)/2$
Longitudinal field energy
0
25
$\omega_p t/2\pi$

Figure 5

NOTICE

This report was prepared as an account of work sponsored by the United States Government. Neither the United States nor the United States Energy Research & Development Administration, nor any of their employees, nor any of their contractors, subcontractors, or their employees, makes any warranty, express or implied, or assumes any legal liability or responsibility for the accuracy, completeness or usefulness of any information, apparatus, product or process disclosed, or represents that its use would not infringe privately-owned rights.

NOTICE

Reference to a company or product name does not imply approval or recommendation of the product by the University of California or the U.S. Energy Research & Development Administration to the exclusion of others that may be suitable.

Printed in the United States of America
Available from
National Technical Information Service
U.S. Department of Commerce
5285 Port Royal Road
Springfield, VA 22161
Price: Printed Copy $; Microfiche $3.00

Page Range	Domestic Price	Page Range	Domestic Price
001–025	$ 3.50	326–350	10.00
026–050	4.00	351–375	10.50
051–075	4.50	376–400	10.75
076–100	5.00	401–425	11.00
101–125	5.50	426–450	11.75
126–150	6.00	451–475	12.00
151–175	6.75	476–500	12.50
176–200	7.50	501–525	12.75
201–225	7.75	526–550	13.00
226–250	8.00	551–575	13.50
251–275	9.00	576–600	13.75
276–300	9.25	601–up	*
301–325	9.75		

*Add $2.50 for each additional 100 page increment from 601 to 1,000 pages; add $4.50 for each additional 100 page increment over 1,000 pages.

Technical Information Department
LAWRENCE LIVERMORE LABORATORY
University of California | Livermore, California | 94550